

1 Auxiliary material for

2  
3 **The multiple fates of sinking particles in the North Atlantic Ocean**

4  
5 James R. Collins<sup>1,2\*</sup>, Bethanie R. Edwards<sup>1,2</sup>, Kimberlee Thamatrakoln<sup>3</sup>, Justin E. Ossolinski<sup>2</sup>,  
6 Giacomo R. DiTullio<sup>4</sup>, Kay D. Bidle<sup>3</sup>, Scott C. Doney<sup>2</sup>, and Benjamin A. S. Van Mooy<sup>2</sup>

7  
8 <sup>1</sup> MIT/WHOI Joint Program in Oceanography/Applied Ocean Science and Engineering, Woods  
9 Hole, MA 02543, USA

10 <sup>2</sup> Department of Marine Chemistry and Geochemistry, Woods Hole Oceanographic Institution,  
11 Woods Hole, MA 02543, USA

12 <sup>3</sup> Department of Marine and Coastal Sciences, Rutgers University, New Brunswick, NJ 08901,  
13 USA

14 <sup>4</sup> Hollings Marine Laboratory, College of Charleston, Charleston, SC 29412, USA

15  
16 **\*To whom correspondence should be addressed:** phone: (508) 289-2627; fax: (508) 457-  
17 2164; e-mail: [jrcollins@whoi.edu](mailto:jrcollins@whoi.edu)

18  
19 Global Biogeochemical Cycles, 2015

20  
21 **Introduction**

22  
23 Contained in this file are three types of Auxiliary Material. The file includes (1) three figures, (2)  
24 two tables, and (3) text describing our remote sensing data analysis and Winkler titration  
25 methods.

26  
27 **Figure S1.** Summary statistics for bacterial production data.

28  
29 **Figure S2** Contour plots of water column bacterial production rates along the two cruise tracks.

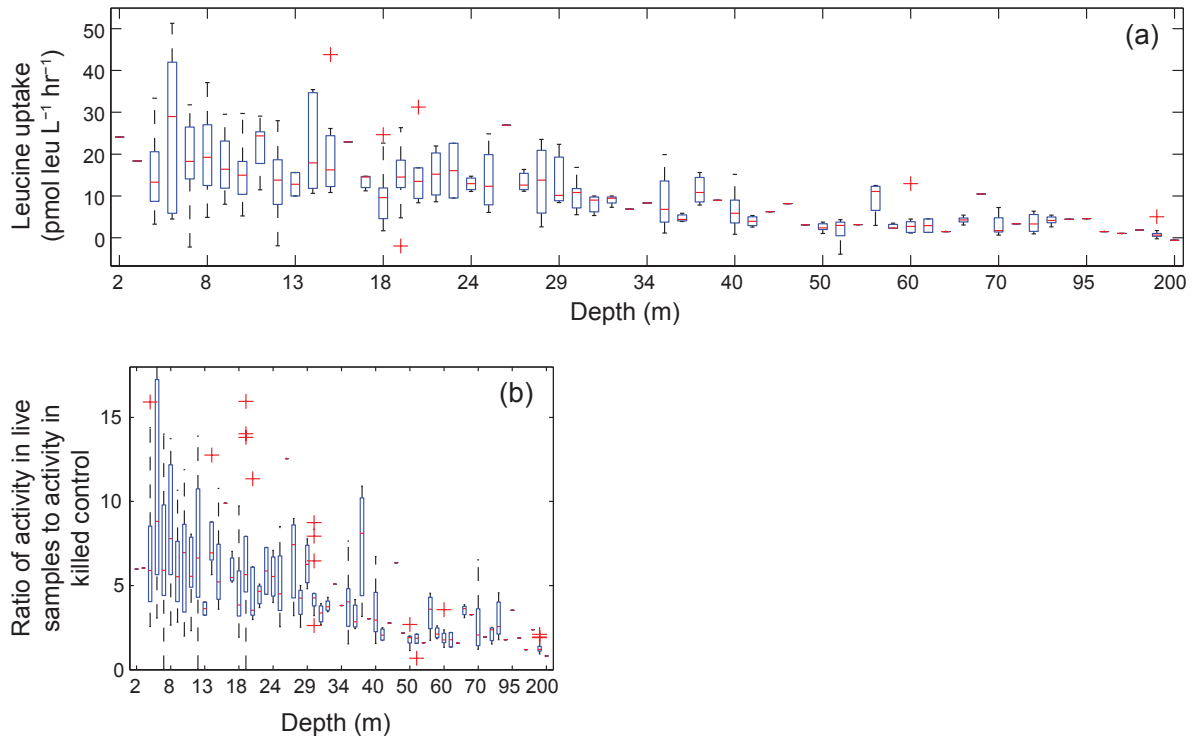
30  
31 **Figure S3.** Mixed layer community respiration rates at four process stations calculated using two  
32 different methods

33  
34 **Table S1.** Tabulation of Average Particle Sinking Velocities ( $W_{avg}$ ) Previously Reported for the  
35 North Atlantic Ocean.

36  
37 **Table S2.** Water Column Respiration Rates Measured in the Mixed Layer Using Two Methods,  
38 April-July 2012..

39  
40 **Remote sensing data.** Description of the MODIS AQUA data we used to generate the surface  
41 reflectance image in Fig. 1b.

42  
43 **Use of Winkler titrations to validate respiration rate calculations.** Text containing a detailed  
44 description of methods.



48

49 **Figure S1.** Summary statistics for bacterial production data. (a) Box-and-whisker plot by depth

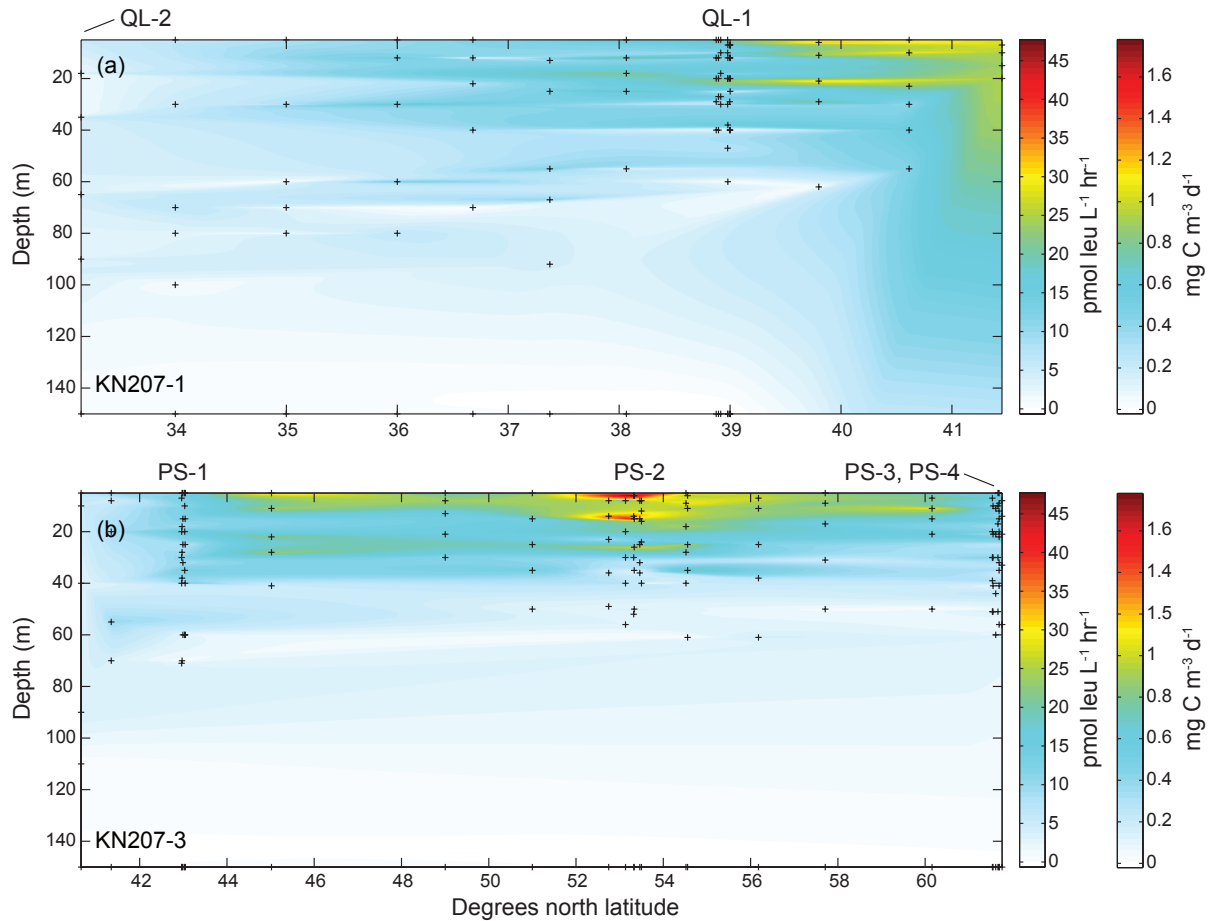
50 of all leucine incorporation observations, corrected for activities in killed control samples. (b)

51 Box-and-whisker plot by depth of the signal-to-noise ratio, i.e., the ratio of the mean of the

52 activity measured in the three live replicates to the activity in the killed control. Red lines

53 represent the median values for each depth, box extremities are the 75<sup>th</sup> and 25<sup>th</sup> quartiles,54 whisker tails are 95<sup>th</sup> and 5<sup>th</sup> quartiles, and red + symbols represent outliers.

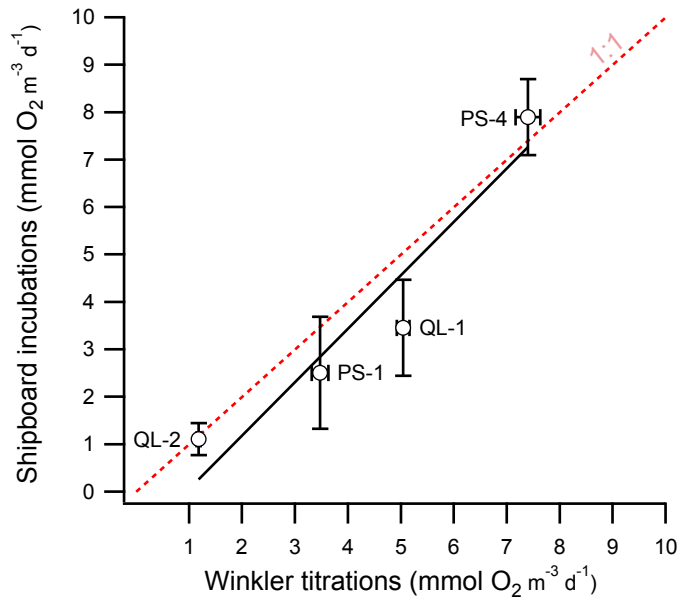
55



56

57 **Figure S2.** Contour plots of water column bacterial production rates measured using the  $^3\text{H}$ -  
 58 leucine incorporation method along the (a) KN207-1 and (b) KN207-3 cruise tracks. Data are  
 59 presented in volumetric units of leucine uptake and in  $\text{mg C m}^{-3} \text{d}^{-1}$ . For conversion to units of C  
 60 in these plots (on secondary axis), an isotope dilution ( $ID$ ) of 1 and a conversion factor  $\nu_{C:leu}$  of  
 61  $1.5 \text{ kg C (mol leu)}^{-1}$  were assumed, making the rates a minimum estimate of bacterial carbon  
 62 turnover. Superimposed (+) are locations of our discrete observations, which we used to generate  
 63 the contour plots. Also superimposed are the locations of the six process stations.

64



65

66 **Figure S3.** Mixed layer community respiration rates at four process stations calculated using two  
 67 different methods. *x*-axis: Rates calculated from a series of 300 mL shipboard incubations using  
 68 optode sensor spots. *y*-axis: Rates calculated using a traditional two-point Winkler titration  
 69 method. A type II (major axis - orthogonal distance) linear regression was fit to the data (solid  
 70 black trace;  $y = 1.13x - 1.07$ ;  $r^2 = 0.95$ ). A 1:1 line (dashed red trace) is superimposed for  
 71 reference. Error bars represent uncertainties from replication (Winkler method) or the standard  
 72 error of regression (incubations).

73

74 **Table S1.** Average Particle Sinking Velocities ( $W_{avg}$ ) Reported for the Mesopelagic Subtropical and Subpolar North Atlantic Ocean<sup>a</sup>

75

Location	Depth or depth range for which reported (m)	Average particle sinking velocities ( $W_{avg}$ ; m d <sup>-1</sup> )	No. individual observations (n) tabulated	Notes	Reference
Bermuda-Atlantic Time Series (BATS) study site, Sargasso Sea (31° 40'N, 64° 10'W)	150-500	13-70	4	Individual observations	McDonnell et al. [2015]
Porcupine Abyssal Plain (PAP) site (48°N, 16.5°W)	50-500	30-250	29	Individual observations; only one observation > 200 m d <sup>-1</sup>	Villa-Alfageme et al. [2014]
Multiple sites along E-W cruise transect from Massachusetts to NW Africa	0-500	0.2-22	22	Individual observations for lithogenic particles from Aeolian inputs	Ohnemus and Lam [2014]
PAP site	50	9 ± 9	—	Mean for slow sinking particle size pool (< 10 m d <sup>-1</sup> )	Riley et al. [2012]
Coastal Norway (60° 16'N 5° 12'E)		181 ± 8	—	Mean for fast sinking pool (> 350 m d <sup>-1</sup> )	Bach et al. [2012]
		9	—	Mean value for all sediment trap material between 80-400 μm	
Canary Current (27° 30'N, 016° 15'W; 27° 30'N, 15° 45'W)	260	12.5 ± 4.8	—	Mean value for fecal pellets	Alonso-González et al. [2010]
		0.7-11	—	Range given for slow-sinking particle fraction comprising ~ 60% of total POC	
POMME study area, NE of Azores (39–45°N, 15–21°W)	< 1000 m	10	—	Mean value estimated for particle size fraction > 100 μm diameter; largely based on observations in mesoscale eddy features	Guidi et al. [2007]
N-S JGOFS cruise transect from NW of Azores (40° 37'N, 20° 5'W) to Iceland (63° 1'N, 22° 25'W)	< 1025 m	137.8-162.5	—	Lower and upper limits for bulk sinking particle material from coccolithophore blooms	Knappertsbusch and Brummer [1995]
		123-156 with $\bar{x} = 141 \pm 11$	6	Estimates for particles from individual coccolithophore species	
NABE site W of Madeira Island (34°N, 21°W)	< 1000 m	46	1	Individual observation	Honjo and Manganini [1993]
NABE site in central N. Atlantic (48°N, 21°W)	< 1000 m	32-116	3	Individual observations	Honjo and Manganini [1993]
Porcupine Seabight (50°N, 13°W)	Surface to deep ocean	100-150	—	Range of values for diatom aggregates	Billett et al. [1983]

76 <sup>a</sup>We restricted our reporting of the literature to values measured for depths < 1000 m for the region between 22°N and 66°N latitude.  
77 From these 9 studies, we gathered 72 individual observations of the average particle sinking velocity; these were used to generate the  
78 histogram in Fig. 5. Where values were reported for multiple depth ranges, we used the observations most applicable to the range of  
79 depths (50-300 m) we evaluated in our study. An extensive compilation of sinking speed data for Atlantic tropical systems (Cape  
80 Blanc, E. and W. Equatorial Atlantic, Benguela Current) and the Southern Ocean can be found in Fischer and Karakas [2009].  
81

82 **Table S2.** Water Column Respiration Rates Measured in the Mixed Layer Using Two Methods, April-July 2012<sup>a</sup>

83

Cruise	Station	Location	Deploy -ment Dates	Euphotic Zone Depth <sup>b</sup> (m)	Depth of Obser- vation (m)	Respiration Rate <sup>c</sup> (mmol O <sub>2</sub> m <sup>-3</sup> d <sup>-1</sup> ± uncertainty)		Method Precision (error as % of rate estimate)	
						Shipboard Incubations <sup>d</sup>	Winkler Titrations <sup>e</sup>	Shipboard Incubations	Winkler Titrations
KN207-1	QL-1	38° 52' 47.4" N, 69° 6' 19.2" W	24-27 Apr 2012	38	29	3.46 ± 1.01	5.04 ± 0.12	29.2%	2.39%
	QL-2	32° 57' 2.4" N, 65° 44' 58.8" W	30 Apr- 3 May 2012	—	14	1.11 ± 0.34	1.18 ± 0.04	30.6%	3.39%
KN207-3	PS-1	43° 1' 58.6" N, 27° 15' 31.8" W	17-19 Jun 2012	58	20	2.51 ± 1.18	3.47 ± 0.16	47.0%	4.73%
	PS-2	53° 29' 43.0" N, 30° 45' 2.6" W	23-27 Jun 2012	26	7	4.03 ± 0.46	—	11.4%	—
	PS-3	61° 37' 9.22" N, 34° 6' 9.64" W	1-5 Jul 2012	42	21.5	2.55 ± 1.11	—	43.5%	—
	PS-4	61° 41' 40.4" N, 33° 46' 21.7" W	7-11 Jul 2012	41	20	7.90 ± 0.80	7.40 ± 0.23	10.1%	2.92%

84 <sup>a</sup>Community respiration rates of free-living microorganisms in unfiltered water samples. Rates from both methods are based on  
85 dissolved oxygen data. For conversion to units of C, a molar respiratory quotient of 117/170 was used.  
86 <sup>b</sup>The depth at which photosynthetically active radiation (PAR) was equal to 1% of surface irradiance, as determined by CTD. We were  
87 unable to obtain PAR data for station QL-2 due to a sensor failure.  
88 <sup>c</sup>We report rates here in volumetric units of dissolved oxygen; to convert to units of  $\text{mg C m}^{-3} \text{ d}^{-1}$ , multiply these rates by the  
89 respiratory quotient (e.g.  $117/170$ )  $\times 12.01 \text{ g mol}^{-1}$ .  
90 <sup>d</sup>Mean of  $\geq 5$  replicates; rate calculated by linear regression of measurements taken at multiple time points in replicate incubations.  
91 Uncertainty is reported as the standard error of regression.  
92 <sup>e</sup>Mean of 3 replicates; rate calculated as difference of titrations at  $t = 0$  and conclusion of incubation. Uncertainty is reported as  
93 standard error.



94 **Remote sensing data analysis**

95 To generate the image in Fig. 1b, we used 8-day average, level 3 MODIS AQUA satellite  
96 data of surface reflectance at 555 nm. A 4 km resolution data file  
97 (A20121772012184.L3m\_8D\_RRS\_Rrs\_555\_4km.hdf) was retrieved using the NASA GSFC  
98 OceanColor Level 3 Browser at <http://oceancolor.gsfc.nasa.gov/cgi/l3>. The false-color image  
99 was generated in ArcGIS 10.1 after geographical indexing.

100

101 **Use of Winkler titrations to validate respiration rate calculations**

102 To validate the water-column respiration rates we derived from our shipboard  
103 incubations, we used a simple method based on a series Winkler titrations. Winkler titration  
104 remains the standard analytical method for determination of dissolved oxygen in water [EPA  
105 Method 360.2 as modified for shipboard determination in seawater; *U S EPA*, 1983]. For the  
106 comparison, we chose the depth in each respiration profile (Fig. 3) that corresponded to the  
107 middle of the mixed layer (Table 3). We determined the respiration rate at this depth using  
108 triplicate samples sacrificed at two timepoints. A  $t = 0$  dissolved oxygen concentration was  
109 determined immediately in samples collected from the same CTD cast used for the respiration  
110 profile. A final concentration was determined using 300 mL samples that had been incubated  
111 alongside the optode sensor spot bottles. The respiration rate was determined by simple  
112 difference of the mean concentrations at the two timepoints.

113

114

115 **References**

- 116 Alonso-González, I. J., J. Arístegui, C. Lee, A. Sanchez-Vidal, A. Calafat, J. Fabrés, P. Sangrá,  
117 P. Masqué, A. Hernández-Guerra, and V. Benítez-Barrios (2010), Role of slowly settling  
118 particles in the ocean carbon cycle, *Geophys. Res. Lett.*, 37(13), L13608,  
119 doi:10.1029/2010GL043827.
- 120 Bach, L. T., U. Riebesell, S. Sett, S. Febiri, P. Rzepka, and K. G. Schulz (2012), An approach for  
121 particle sinking velocity measurements in the 3-400  $\mu\text{m}$  size range and considerations on the  
122 effect of temperature on sinking rates, *Mar. Biol.*, 159(8), 1853-1864, doi:10.1007/S00227-012-  
123 1945-2.
- 124 Billett, D. S. M., R. S. Lampitt, A. L. Rice, and R. F. C. Mantoura (1983), Seasonal  
125 sedimentation of phytoplankton to the deep-sea benthos, *Nature*, 302(5908), 520-522.
- 126 Fischer, G., and G. Karakas (2009), Sinking rates and ballast composition of particles in the  
127 Atlantic Ocean: implications for the organic carbon fluxes to the deep ocean, *Biogeosciences*,  
128 6(1), 85-102.
- 129 Guidi, L., L. Stemann, L. Legendre, M. Picheral, L. Prieur, and G. Gorsky (2007), Vertical  
130 distribution of aggregates ( $> 110 \mu\text{m}$ ) and mesoscale activity in the northeastern Atlantic:  
131 Effects on the deep vertical export of surface carbon, *Limnol. Oceanogr.*, 52(1), 7-18.
- 132 Honjo, S., and S. J. Manganini (1993), Annual Biogenic Particle Fluxes to the Interior of the  
133 North-Atlantic Ocean - Studied at 34-Degrees-N 21-Degrees-W and 48-Degrees-N 21-Degrees-  
134 W, *Deep-Sea Res Pt II*, 40(1-2), 587-607, doi:10.1016/0967-0645(93)90034-K.
- 135 Knappertsbusch, M., and G. J. A. Brummer (1995), A sediment trap investigation of sinking  
136 coccolithophorids in the North Atlantic, *Deep Sea Research Part I: Oceanographic Research*  
137 *Papers*, 42(7), 1083-1109, doi:10.1016/0967-0637(95)00036-6.
- 138 McDonnell, A. M. P., P. W. Boyd, and K. O. Buesseler (2015), Sinking velocities and microbial  
139 respiration rates alter the attenuation of particulate carbon fluxes through the mesopelagic zone,  
140 *Global Biogeochem. Cycles*, 2014GB004935, doi:10.1002/2014GB004935.
- 141 Ohnemus, D. C., and P. J. Lam (2014), Cycling of lithogenic marine particles in the US  
142 GEOTRACES North Atlantic transect, *DSR*, doi:10.1016/j.dsr2.2014.11.019.
- 143 Riley, J. S., R. Sanders, C. Marsay, F. A. C. Le Moigne, E. P. Achterberg, and A. J. Poulton  
144 (2012), The relative contribution of fast and slow sinking particles to ocean carbon export,  
145 *Global Biogeochem. Cycles*, 26(1), GB1026, doi:10.1029/2011GB004085.
- 146 U.S. Environmental Protection Agency (1983), Oxygen, dissolved (modified Winkler, full-bottle  
147 technique), Method #360.2, Washington, D.C.
- 148 Villa-Alfageme, M., F. de Soto, F. A. C. Le Moigne, S. L. C. Giering, R. Sanders, and R. García-  
149 Tenorio (2014), Observations and modeling of slow sinking particles in the twilight zone, *Global*  
150 *Biogeochem. Cycles*, 28(11), 1327-1342, doi:10.1002/2014GB004981.

151  
152